Journal of Materials Chemistry C

Accepted Manuscript

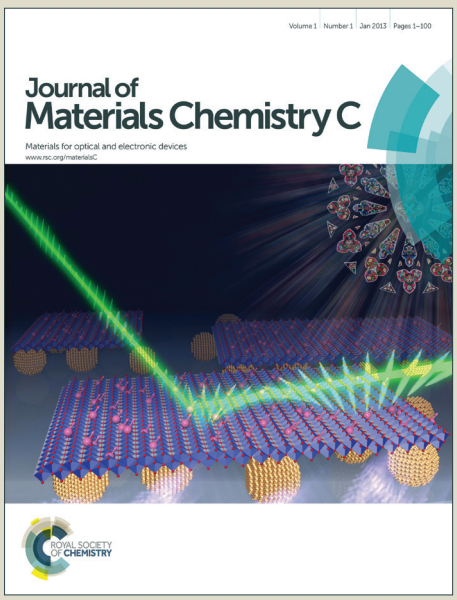

ROYAL SOCIETY OF CHEMISTRY

www.rsc.org/materialsC

Journal Name

RSCPublishing

ARTICLE

Strong blue emissive nanofibers constructed from benzothizole modified *tert*-butyl carbazole derivative for the detection of volatile acid vapors

Cite this: DOI: 10.1039/xoxxoooooox

Received ooth January 2012,
Accepted ooth January 2012

DOI: 10.1039/xoxxoooooox

www.rsc.org/

Jiabao Sun,[a] Pengchong Xue,[a] Jingbo Sun,[a] Peng Gong,[a] Panpan Wang[a] and Ran Lu[a*]

Two new benzothizole modified carbazole derivatives (**CBT** and **TCBT**) were synthesized. It was found that **TCBT** with *tert*-butyl moiety could gel cyclohexane, cyclopentanol and octane/cyclohexane (v/v = 2/1) under ultrasound stimulus, but **CBT** without *tert*-butyl group failed to form organogel in the selected solvents, revealing that *tert*-butyl played an important role in gel formation. X-ray diffraction pattern of xerogel indicated that **TCBT** molecules self-assembled into a lamellar structure in the gel state. In particular, xerogel-based film of **TCBT** emitted strong blue light and could be used as fluorescent sensory materials to detect acid vapors of TFA, HCl, HNO_3, formic acid and acetic acid with high performance on account of the good adsorption and diffusion of analysts in 3D networks as well as the efficient exciton migration in nanofibers. It suggested that the organogelation of π-gelators was a facile way to generate efficient chemosensors.

Introduction

In recent years, organogels formed from low molecular mass gelators have been attracting increasing attentions on account of their numerous practical applications in optoelectronic devices,[1] field-effect transistors[2] and chemosensors, etc.[3] It is known that the gelator molecules aggregate into various nanoscale superstructures through non-covalent interactions, which are sensitive to external chemical or physical factors, such as metal ions, anions, small organic compounds, light irradiation, sound, and mechanical force.[4] Thus, a number of stimulus-active functional organogels have been generated to be used as sensory materials.[5] However, the sensitivity is often low if the sensory process is based on gel-sol transition. Recently, the fluorescent nanofibers-based xerogels fabricated from π-gelators have been employed as fluorescent sensors to detect some toxic or explosives vapors with rapid response and high sensitivity because the high surface-to-volume ratios and the 3D networks make easy adsorption and diffusion of the analytes in xerogels.[6]

However, traditional stimulus-responsive gelators usually contain H-bonded units (such as amide, amino acid or urea moieties) and auxiliary groups of long alkyl chain, sugar or cholesterol,[7] which leads to low atom economy and tedious synthetic processes. In addition, the domain formed by long carbon chains would block the information transformation between conjugated systems. Up to date, a series of non-traditional organogels without the above classical auxiliary groups have been synthesized. For example, we have found that *tert*-butyl and triphenylamine groups can replace long alkyl chains to lead to the gel formation directed by balanced π-π interaction.[8] We also designed an asymmetric coplanar gelator of N-methyl carbazole modified benzoxazole and the gel exhibited enhanced emission.[9] Park *et al*. introduced CN or/and CF_3 into stilbene to help molecules self-assemble into nanowires through CH···F and π–π interactions.[10] Würthner found a contortive perylene bisimide-based gelator lacking flexible alkyl chains.[11] Severin demonstrated that organogel-based networks could be obtained by connection of boronate esters through B-N bonds.[12] However, the non-traditional gels used as chemosensors are rare reported.[13] Herein, we designed and synthesized two benzothizole modified carbazole and *tert*-butyl-carbazole derivatives **CBT** and **TCBT** (Scheme 1). It was found that **TCBT** could gelate some solvents, such as cyclohexane, cyclopentanol and octane/cyclohexane (v/v = 2/1) under ultrasound stimulus, while **CBT** could not form gel in the selected solvents, suggesting that *tert*-butyl group played a vital role in the gel formation. X-ray diffraction pattern of xerogel **TCBT** revealed a lamellar packing of the gelator molecules in gel state. It should be noted that the yellowish wet gel of **TCBT** emitting strong fluorescence could transfer into orange solution upon the addition of TFA, accompanying with the obvious red-shift and decreasing of the emission. Notably, the strong blue emission of the xerogel film based on **TCBT** was quenched significantly upon exposed to gaseous acids, and the xerogel film could quantitatively detect acid vapors, such as TFA, HCl, formic, HNO_3 et al. This work will help us to design novel non-

traditional gelators and fabricate luminescent nanofibers used as chemosensors with high performance.

Experimental

Materials

Toluene and THF was freshly distilled from sodium and benzophenone. Other chemicals were used as received.

Measurement and characterization

^{1}H and ^{13}C NMR spectra were recorded on a Bruker-Avance III (400 MHz and 125 MHz) spectrometer with $CDCl_3$ as solvent and tetramethylsilane (TMS) as the internal standard. FT-IR spectra were recorded with a Nicolet-360 FT-IR spectrometer by the incorporation of samples into KBr disks. Mass spectra were obtained with AXIMA CFR MALDI-TOF (Compact) mass spectrometers. The UV-vis absorption spectra were obtained using a Mapada UV-1800pc spectrophotometer. Photoluminescence measurements were taken on a Cary Eclipse fluorescence spectrophotometer. The fluorescence quantum yield of **TCBT** in cyclohexane was measured by comparing to a standard (quinine sulfate in 1 N H_2SO_4 aqueous solution, Φ_F = 0.65). The excitation wavelength was 365 nm. The fluorescence quantum yield of **TCBT** in xerogel phase was measured on an Edinburgh FLS920 steady state spectrometer using an integrating sphere. Scanning electron microscopy (SEM) images were obtained on a JEOL JSM-6700F (operating at 3 kV). The samples for SEM measurements were prepared by casting the organogel on silicon wafers and drying at room temperature, followed by coating with gold. Fluorescence microscopy images were recorded on a Fluorescence Microscope (Olympus Reflected Fluorescence System BX51, Olympus, Japan). X-ray diffraction pattern was obtained on a Japan Rigaku D/max-γA. XRD equipped with graphite monochromatized Cu Kαradiation (λ=1.5418 Å), employing a scanning rate of 0.02 °s^{-1} in the 2θ range of 1° to 30°. The samples for fluorescence microscopy and XRD measurements were prepared by casting the gels onto a glass slide and drying at room temperature. The molecular optimal configurations were used to obtain the frontier orbitals of **TCBT** by density functional theory (DFT) calculations at B3LYP/6-31G(d) level with the Gaussian 09W program package.[14]

Single crystals of **CBT** were obtained in the mixture of CH_2Cl_2 and hexane by a slow solvent diffusion method, and were selected for X-ray diffraction studies in a Rigaku RAXIS-RAPID diffractometer using graphite-monochromated MoK_α radiation (λ = 0.71073 Å). The crystals were kept at room temperature during the data collection. The structures were solved by direct methods and refined on F^2 by full-matrix least-square using the SHELXTL-97 Program.[15] The C, N, O, and S atoms were easily placed from the subsequent Fourier-difference maps and refined anisotropically.

Synthesis of CBT and TCBT

Synthetic routes for **CBT** and **TCBT** were shown in Scheme 1. 4-(9H-carbazol-9-yl)benzaldehyde and 4-(3,6-di-tert-butyl-9H-carbazol-9-yl)benzaldehyde were prepared according to the methods reported previously.[16]

(E)-2-(4-(9H-carbazol-9-yl)styryl)benzo[d]oxazole (CBT). Potassium *tert*-butoxide (0.17 g, 1.5 mmol) was dispersed in dry THF (10 mL), which was stirred at 0 ℃ for 10 min. Then, 2-methylbenzo[d]thiazole (0.14 mL, 1.2 mmol) was added into the mixture slowly. After stirred at 0 ℃ for 30 min, the solution of **2** in THF (0.27 g, 10 mL**)** was added dropwise. After stirred for another 2 h the mixture was poured into water (300 mL). The precipitates was filtered and washed with water. The residue was purified by column chromatography using dichloromethane as an eluent to afford **CBT** (0.33 g, 84%) as yellow powder. Mp: 210.0–212.0 °C. ^{1}H NMR (400 MHz, $CDCl_3$) δ 8.18 (d, *J* = 7.7 Hz, 2H), 8.11 (d, *J* = 8.0 Hz, 1H), 7.93 (d, *J* = 7.4 Hz, 1H), 7.87 (d, *J* = 8.4 Hz, 2H), 7.74 (d, *J* = 16.2 Hz, 1H), 7.68 (d, *J* = 8.4 Hz, 2H), 7.62 – 7.42 (m, 7H), 7.38 – 7.31 (m, 2H). ^{13}C NMR (125 MHz, $CDCl_3$): *δ* (ppm) = 166.74, 153.88, 140.53, 138.67, 136.59, 134.28, 128.83, 127.23, 126.53, 126.11, 125.58, 123.65, 123.03, 122.58, 121.61, 120.42, 120.31, 109.84, 99.89. FT-IR (KBr, cm^{-1}): 2920, 2362, 1650, 1519, 1451, 1228, 750, 720. MS, m/z: calc.: 402.1, found: 403.9 [M + H]$^+$.

(E)-2-(4-(3,6-di-*tert*-butyl-9H-carbazol-9-yl)styryl)benzo[d]thiazole (TCBT). By following the synthetic procedure for **CBT**, **TCBT** was synthesized using compound **4** (0.38 g, 1 mmol) as reagent. The crude product was purified by column chromatography using dichloromethane as an eluent to afford **TCBT** (0.43 g, 85%) as yellow powder. Mp: 246.0–247.0 °C. ^{1}H NMR (400 MHz, $CDCl_3$) *δ* (ppm): 8.17 (s, 2H), 8.13 (d, *J* = 8.2 Hz, 1H), 7.93 (d, *J* = 7.9 Hz, 1H), 7.85 (d, *J* = 8.3 Hz, 2H), 7.77 (d, *J* = 16.2 Hz, 1H), 7.67 (d, *J* = 8.4 Hz, 2H), 7.62-7.44 (m, 7H), 1.50 (s, 18H). ^{13}C NMR (125 MHz, $CDCl_3$) *δ* (ppm): 169.66, 166.87, 143.28, 139.27, 138.85, 136.86, 133.71, 128.79, 126.76, 126.52, 125.55, 123.75, 123.65, 122.94, 122.20, 121.59, 116.33, 109.30, 99.93, 34.75, 32.02. FT-IR (KBr, cm^{-1}): 2958, 2862, 1610, 1514, 1473, 1369, 194, 758. MS, m/z: calc.: 514.2, found: 515.7 [M + H]$^+$.

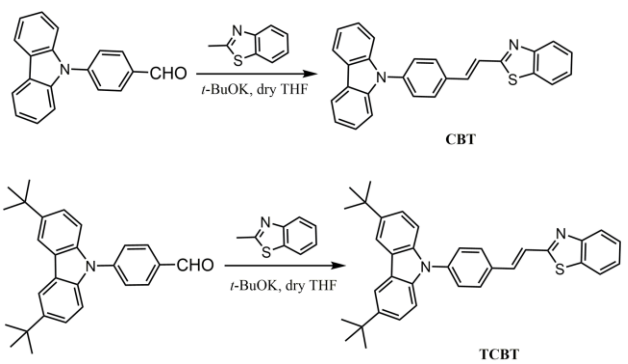

Scheme 1. The synthetic routes for **CBT** and **TCBT**.

Results and discussion

Synthesis of compounds CBT and TCBT

The synthetic routes for compounds **CBT** and **TCBT** were shown in Scheme 1. Firstly, 4-(9H-carbazol-9-yl)benzaldehyde and 4-(3,6-di-tert-butyl-9H-carbazol-9-yl)benzaldehyde were prepared according to the methods reported previously.[16] Then, the target compounds of **CBT** and **TCBT** was prepared via Knoevenagel condensation reaction of 2-methylbenzo[d]thiazole with 2-methyl benzoxazole and 4-(9H-carbazol-9-yl)benzaldehyde or 4-(3,6-di-tert-butyl-9H-carbazol-9-yl)benzaldehyde, respectively, catalyzed by *t*-BuOK in yield of ca. 84%. **CBT** and **TCBT** were characterized by ^{1}H NMR, ^{13}C NMR and MALDI-TOF MS. In addition, we gained the single crystal of **CBT** by the slow solvent-diffusion method. X-ray single crystal diffraction revealed that the dihedral angle between carbazole group and adjacent phenyl moiety was 49.64° (Figure S1). The dihedral angle between benzothiazole and adjacent phenyl was estimated to be ca. 5.74°, revealing good coplanar. In the single crystal of **CBT**, molecules packed into one-dimensional aggregates, and the slipping angle was calculated to be 32.63°, suggesting the formation of *J*-aggregates.

Gelation abilities of CBT and TCBT

The gelation properties of **CBT** and **TCBT** were tested in various solvents by means of the "stable to inversion of a test tube" method.[17] As summarized in Table 1, **TCBT** was not dissolved in hexane and petroleum ether. It was soluble in cyclohexane, octane and the mixture of octane and cyclohexane upon heating, but only precipitate was observed in these solvents as cooled to room temperature. Fortunately, when the hot solutions in cyclohexane, cyclopentanol and octane/cyclohexane (v/v = 2/1) was treated by ultrasound stimulus for 15 s and rested at room temperature for 10 min, tough gels formed. However, the gel could not be formed from **CBT** under heating/cooling or ultrasound treatments. **CBT** was insoluble in apolar solvents, such as hexane, cyclohexane and octane even upon heating. Precipitate was separated from the hot toluene, cyclopentanol, and *n*-butanol solutions of **CBT**. The two compounds showed good solubility in $CHCl_3$, DMF and DMSO. The above results suggested *tert*-butyl played a vital role in the gel formation of benzothizole modified carbazole derivatives because it could tune the strength of π–π interaction.[8a]

Table 1 Gelation abilities of **CBT** and **TCBT** in organic solvents.[a]

Solvent	CBT	TCBT (CGC)
Hexane	I	I
Cyclohexane	I	G (3.1)
Octane	I	P
Octane/Cyclohexane (v/v = 2/1)	I	G (5.0)
Petroleum ether	I	I
Toluene	P	P
Chloroform	S	S
Ethanol	I	I
Cyclopentanol	P	G (11.3)
n-Butanol	P	P
DMF	S	S
DMSO	S	S

[a] I: insoluble; S: soluble; G: stable gel; P: precipitate. CGC: critical gelation concentration (mg/mL)

Self-assembly of TCBT in gel phase

The morphologies of the organogels were determined by SEM. As shown in Figure 1, gelators **TCBT** self-assembled into nanofibers with a diameter of 50-200 nm in cyclohexane and a 3D network was constructed by numerous intertwined slender nanofibrils. Such 3D network with 1D nanostructures as well as high interspace will be favorable for the absorption and diffusion of gas molecules.[18]

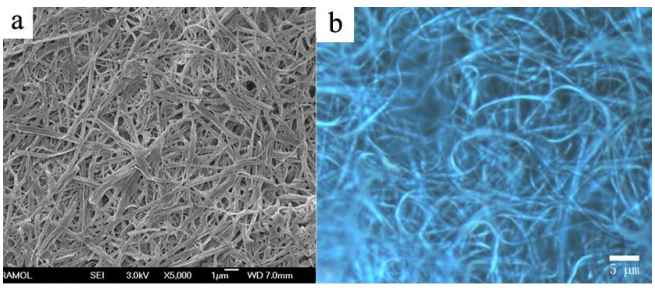

Figure 1. (a) SEM and (b) fluorescence microscopy (λ_{ex} = 365 nm) images of xerogel **TCBT** obtained from cyclohexane.

In order to investigate the intermolecular interaction during gel formation, the time-dependent UV-vis absorption and fluorescent emission spectra of **TCBT** in cyclohexane (8.0×10^{-3} M) upon cooling the hot solution, which was first stimulated by ultrasound, to room temperature were measured. As shown in Figure 2a, we found that during the gelation process the absorption bands in the range of 275-305 nm for **TCBT** decreased gradually, and the intensity of the absorption above 425 nm increased gradually. An isosbestic point at 415 nm appeared. In addition, the dilute cyclohexane solution of **TCBT** gave absorption at 377 nm, which red-shifted to 386 nm in xerogel-based film (Figure S2). Thus, we suggested that π-π interaction between the aromatic moieties had an effect on the formation of gels.[19] The fluorescence emission spectrum of **TCBT** in cyclohexane showed two peaks at 414 nm and 440 nm, which increased gradually during gel formation (Figure 2b). The fluorescence quantum yields of **TCBT** in cyclohexane solution and xerogel phase were 0.34 and 0.47, respectively. The relative high fluorescence emission of **TCBT** would be benefit for sensing analytes via monitoring the changes of the emisison.[20]

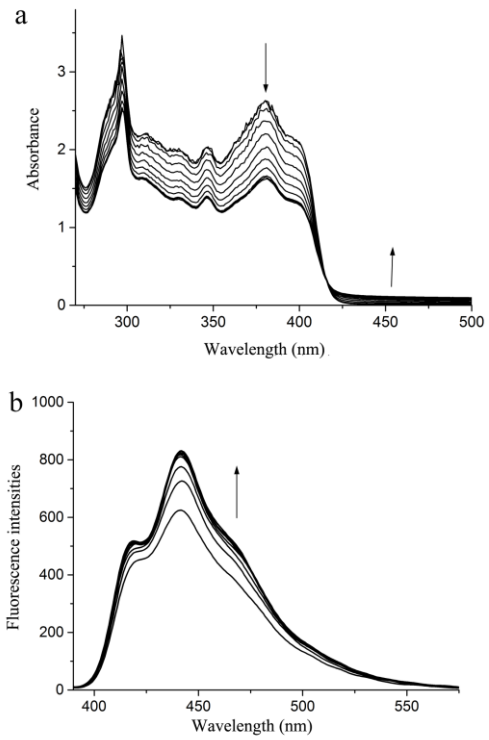

Figure 2. Time-dependent UV-vis absorption (a) and fluorescence emission (b, λ_{ex} = 380 nm) spectra of **TCBT** upon cooling the hot solution in cyclohexane (8.0×10^{-3} M), which was first stimulated by ultrasound to room temperature. The alternation is 15 s. The arrows indicate the spectral changes from the sol to gel.

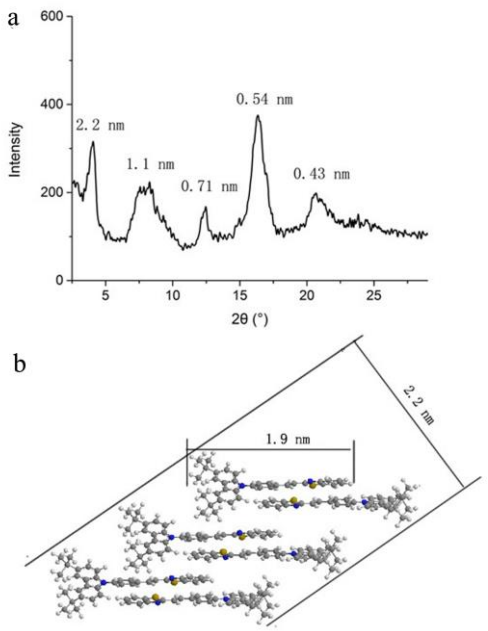

Figure 3. (a) X-ray diffraction pattern of the xerogel of **TCBT** obtained from cyclohexane and (b) schematic illustration of the layered structure in the gel of **TCBT** with a period of 2.2 nm.

XRD pattern of xerogel **TCBT** gave the diffraction peaks at *d*-spacing of 2.2 nm, 1.1 nm and 0.71 nm, respectively (Figure 3a). They are in the ratio of ca. 1/1:1/2:1/3, suggesting that a lamellar organization with a long period of 2.2 nm was generated from **TCBT** in the gel state.[21] Moreover, the molecular length of **TCBT** in optimized geometry based on DFT calculations was 1.9 nm (Figure 3b), which was shorter than the lamellar period obtained by XRD pattern of the xerogel. Therefore, we deduced that **TCBT** might packed into an anti-parallel bimolecular layered structure in the gel state (Figure 3b).

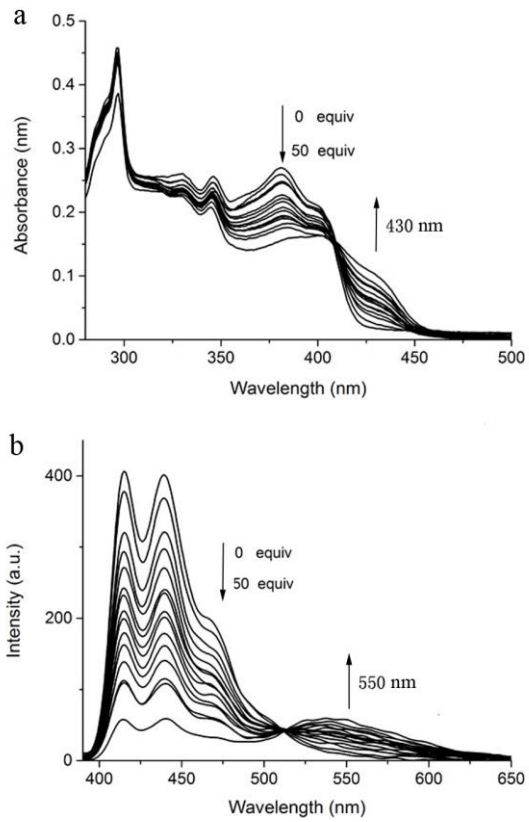

Figure 4. (a) UV-vis absorption and (b) fluorescence emission spectral changes of **TBCT** in cyclohexane (2.0×10^{-5} M) upon addition of different amounts of TFA at 20 °C (λ_{ex} = 380 nm).

Sensory properties of TCBT in organogel and in xerogel-based film towards acids

The spectral response ability of **TCBT** towards TFA in solution was firstly studied. As shown in Figure 4a, the absorption band in the range of 350-400 nm for **TCBT** in cyclohexane decreased gradually and new absorption band located at 430 nm appeared and intensified with increasing amount of TFA. We could find an isometric point at 410 nm, meaning the formation of new species. We deemed that the benzothiazole unit might be protonated by TFA. Because the increased electron-withdrawing ability of protonated benzothiazole, a new red-shifted absorption band appaered.[22] Meanwhile, the

colourless solution converted into a pale yellow one. The fluorescence spectral change of **TCBT** upon the addition TFA was shown in Figure 4b. It was clear that the emission bands located at 415 nm and 440 nm decreased gradually with an increase in the concentration of TFA and a new weak emission at 550 nm emerged. The strong blue emission of **TCBT** could be quenched significantly by TFA. Therefore, **TCBT** could be used as a probe to detect TFA by naked eyes.

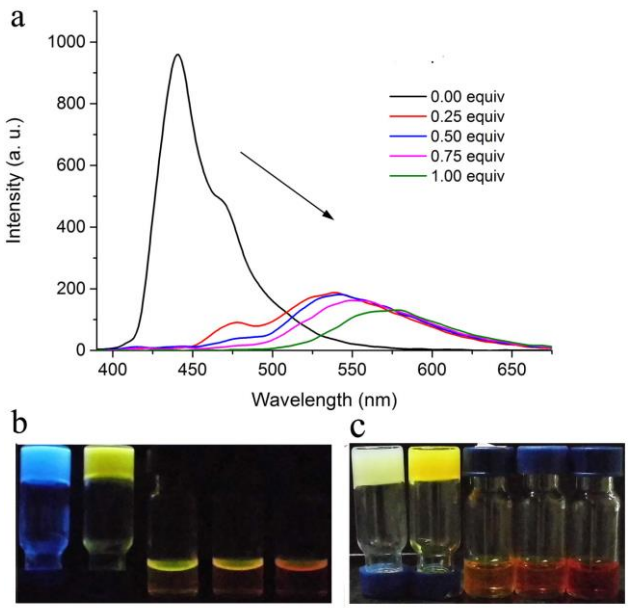

Figure 5. (a) Fluorescence emission spectra of **TCBT** in cyclohexane (7.8×10^{-3} M) upon the addition of TFA (λ_{ex} = 380 nm). Photographs of the **TCBT** in cyclohexane containing different amount of TFA (b) under 365 nm light and (c) under daylight (from left to right, the amount of TFA was 0.00, 0.25, 0.50, 0.75 and 1.00 equiv., respectively).

The wet organgel of **TCBT** could also act as a sensor for probing TFA. As shown in Figure 5a and 5b, the neat gel emitted strong blue fluorescence located at 435 nm. Upon the addition of 0.25 equiv. of TFA, the gel gave yellow emission with a maximum at 539 nm. When 1 equiv. of TFA was added, the formed solution exhibited a weak emission with a maximum at 575 nm. At the same time, we found that the neat cyclohexane gel of **TCBT** was white. When 0.25 equiv. of TFA was added into the organogel **TCBT**, yellow gel appeared. When 0.5 equiv. of TFA was added, the organogel was destroyed, and the orange red solution was observed (Figure 5c). Further adding TFA, the solution turned into red. Thus, the organogel could also sense acid by naked eyes.

It is well known that the luminescent nanofibers-based films usually show more sensitive response to analytes due to the high specific surface area as well as efficient exciton migration in the nanofibers.[23] Herein, the nanofibers-based film of **TCBT** was expected to detect volatile acid vapors. As shown in Figure 6a, the emission intensity at 457 nm for the xerogel-based film of **TCBT** decreased obviously upon exposed to TFA vapor. The higher was the concentration of TFA vapor, the high was the fluorescence quenching efficiency. For example, the quenching efficiency reached 85% when the concentration of TFA vapor was 1600 ppm, at the same time, the response time was short as 1.61 s (Figure 6b). To demonstrate the sensitivity of the xerogel-based film of **TCBT** in sensing gaseous TFA, the concentration-dependent fluorescence quenching efficiency ($1-I/I_0$) was shown in the inset of Figure 6a. A well linear relationship between the quenching efficiencies and the TFA vapor concentration was observed when the concentration is below 200 ppm. The detection limit of the xerogel-based film of **TCBT** could be estimated to be ca. 1.5 ppm towards TFA vapor.[24] Therefore, such xerogel-based film could detect TFA vapor quantitatively.

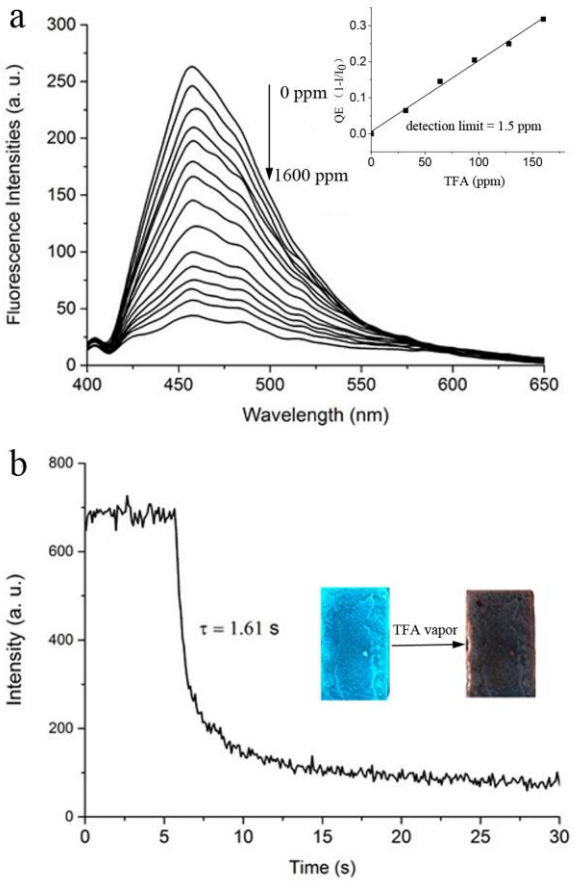

Figure 6. a) Fluorescence emission spectra of **TCBT** in xerogel-based film upon exposed to different amount of TFA vapor (λ_{ex} = 380 nm). Inset: the concentration-dependent fluorescence quenching efficiencies of the film exposed to different amount of TFA vapor for 2 s. b) Time-course of fluorescence quenching of the film upon exposed to TFA vapor at 1600 ppm, and the intensity was monitored at 457 nm. Inset: photo of the xerogel-based film before and after exposed to the TFA vapor under 365 nm light.

The UV-vis absorption spectra of **TCBT** in xerogel-based film upon exposed to different amount of TFA vapor was

measured to explain the fluorescence quenching mechanism (Figure S3). We found that the absorption band located at 388 nm for **TCBT** decreased gradually and a new broad absorption at 464 nm which ascribed to protonated **TCBT** emerged upon exposed to TFA vapor. It was worth noting that only slightly changes of the absorption were detected when the concentration of TFA vapor was maintained at 1600 ppm. This result suggested that a small amount of **TCBT** molecules were protonated by TFA. However, the fluorescence quenching efficiency was more than 85% under the same condition. We deemed that the fluorescence quenching was amplified in the gel nanofibers. It was reasonable to guess that one protonated **TCBT** molecule could act as energy acceptor to quench the emission of many **TCBT** molecules owing to exciton diffusion in the gel nanofibers.[25] It should be noted that new emission band at ca. 550 nm emerged when TFA was added to the diluted solution or the wet gel of **TCBT** (Figure 4b and 5a) on account of the formation of protonated **TCBT**. However, fluorescence quenching of **TCBT** in xerogel-based film was only observed upon exposed to TFA vapor. The reason might be that the emission band of **TBCT** in the xerogel-based film was broadened significantly, and it appeared in the range of 420-600 nm. Upon exposed to TFA vapor, the intensity of the broad emission band decreased. As a result, the edge band at ca. 550 nm also decreased. Therefore, it is difficult to figure out the weak emission of protonated **TBCT** in the film.

We found that the fluorescence of **TCBT** in xerogel-based film could also be quenched upon exposure to other volatile acids of HCl, HNO_3, formic acid and acetic acid (Figures S4-S7). For example, upon exposure of xerogel-based film of **TCBT** to gaseous HCl, the fluorescence intensity of the film gradually decreased with increase of HCl vapor concentration (Figure S4). The detection limit for HCl vapor was determined to be 5.2 ppm. It illustrated that the xerogel-based film can be used as a sensing material to detect volatile acid vapors.

Conclusions

In conclusion, benzothizole modified carbazole and *tert*-butyl-carbazole **CBT** and **TCBT** were synthesized. The gelation abilities of the two compounds in different solvents revealed that **TCBT** with *t*-butyl moiety could gelate cyclohexane, cyclopentanol and octane/cyclohexane (v/v = 2/1) under ultrasound stimulus, but no gel could be formed from **CBT**. It suggested that *t*-butyl played a key role in the gel formation since it could tune the strength of π-π interaction and increase the molecular solubility. It was interesting that **TCBT** exhibited strong fluorescence in wet organogel and in xerogel-based film, and the emission was sensitive to acids. For example, the organogel emitting strong blue light could turn into the gel emitting yellow light when 0.25 equiv. of TFA was added, and further turn into solution with weak emission when more than 0.5 equiv. of TFA was added. The blue emission of the xerogel-based film of **TCBT** could be quenched significantly upon exposed to TFA vapor. When the concentration of TFA vapor was maintained at 1600 ppm, the response time was short as 1.61 s. The detection limit of the film towards gaseous TFA was ca. 1.5 ppm. We deemed that the high performance of xerogel-based film of **TCBT** in probing TFA vapor was originated from the good adsorption and diffusion of analysts in 3D networks consisting lots of nanofibers as well as the efficient exciton migration in 1D nanofibers. Moreover, the xerogel-based film of **TCBT** could also act as fluorescence sensory material in detecting other volatile acids of HCl, HNO_3, formic acid and acetic acid. This work will be helpful in the design of non-traditional π-gelators and fabrication of fluorescence chemosensors with high performance.

Acknowledgements

This work was supported by the National Natural Science Foundation of China (21374041), Open Project of State Key Laboratory of Supramolecular Structure and Materials (SKLSSM2015014).

Notes and references

State Key Laboratory of Supramolecular Structure and Materials, College of Chemistry, Jilin University, Changchun, P. R. China. E-mail: luran@mail.jlu.edu.cn

† Electronic Supplementary Information (ESI) available: ^{1}H NMR, ^{13}C NMR and MALDI/TOF MS spectra of target molecules; Absorption spectra of **TCBT** in solution state and xerogel-based film; Absorption spectra of **TCBT** in xerogel films upon exposure to different amount of TFA vapor; Fluorescence emission spectra of **TCBT** in xerogel films upon exposure to different amount of HCl, HNO_3, formic acid and acetic acid vapors. CCDC 1407672 (**CBT**) and crystallographic data in CIF or other electronic format see DOI: 10.1039/b000000x/

1 a) R. J. Kumar, J. M. MacDonald, T. B. Singh, L. J. Waddington and A. B. Holmes, *J. Am. Chem. Soc.*, 2011, **133**, 8564–8573; b) C. Vijayakumar, V. K. Praveen and A. Ajayaghosh, *Adv. Mater.*, 2009, **21**, 2059–2063.

2 a) J. P. Hong, M. C. Um, S. R. Nam, J. I. Hong and S. Lee, *Chem. Commun.*, 2009, 310–312; b) W. W. Tsai, I. D. Tevis, A. S. Tayi, H. Cui and S. I. Stupp, *J. Phys. Chem. B*, 2010, **114**, 14778–14786; c) D. A. Stone, A. S. Tayi, J. E. Goldberger, L. C. Palmera and S. I. Stupp, *Chem. Commun.*, 2011, **47**, 5702–5704; d) S. Diring, F. Camerel, B. Donnio, T. Dintzer, S. Toffanin, R. Capelli, M. Muccini and R. Ziessel, *J. Am. Chem. Soc.*, 2009, **131**, 18177–18185; e) R. Marty, R. Nigon, D. Leite and H. Frauenrath, *J. Am. Chem. Soc.*, 2014, **136**, 3919–3927.

3 a) N. Yan, Z. Xu, K. K. Diehn, S. R. Raghavan, Y. Fang and R. G.Weiss, *J. Am. Chem. Soc.*, 2013, **135**, 8989–8999; b) S. S. Babu, S. Prasanthkumar and A. Ajayaghosh, *Angew. Chem., Int. Ed.*, 2012, **51**, 1766–1776; c) Z. Zhao, J. W. Y. Lam and B. Z. Tang, *Soft Matter*, 2013, **9**, 4564–4579.

4 a) X. Wang, P. Duan and M. Liu, *Chem. Commun.*, 2012, 48, 7501–7503; b) P. Xue, J. Sun, Q. Xu, R. Lu, M. Takafuji and H. Ihara, *Org. Biomol. Chem.*, 2013, **11**, 1840–1847; c) K. Ghosh, D. Kar, S. Panja and S. Bhattacharya, *RSC Adv.*, 2014, **4**, 3798–3803; d) G. Qing, X. Shan, W. Chen, Z. Lv, P. Xiong and T. Sun, *Angew. Chem. Int. Ed.*, 2014, **53**, 2124–2129; e) K. Sugiyasu, N. Fujita, M. Takeuchi, S. Yamada and S. Shinkai, *Org. Biomol. Chem.*, 2003, **1**, 895–899; f) X. Cao, A. Gao, H. Lv, Y. Wu, X. Wang and Y. Fan, *Org. Biomol. Chem.*, 2013, **11**, 7931–7937.

5 S. S. Babu, V. K. Praveen and A. Ajayaghosh, *Chem. Rev.*, 2014, **114**, 1973–2129.
6 a) X. L. Liu, X. F. Zhang, R. Lu, P. C. Xue, D. F. Xu and H. P. Zhou, *J. Mater. Chem.*, 2011, **21**, 8756–8765. b) C. Y. Bao, R. Lu, M. Jin, P. C. Xue, C. H. Tan, G. F. Liu and Y. Y. Zhao, *Chem. Eur. J.*, 2006, **12**, 3287–3294.
7 a) L. E. Buerklea and S. J. Rowan, *Chem. Soc. Rev.*, 2012, **41**, 6089–6102; b) S. Bhattacharya and S. K. Samanta, *Langmuir*, 2009, **25**, 8378–8381; c) H. Jintoku, M. Takafuji, R. Oda and H. Ihara, *Chem. Commun.*, 2012, **48**, 4881–4883.
8 a) X. C. Yang, R. Lu, T. H. Xu, P. C. Xue, X. L. Liu and Y. Y. Zhao, *Chem. Commun.*, 2008, 453–455; b) X. C. Yang, R. Lu, F. Y. Gai, P. C. Xue and Y. Zhan, *Chem. Commun.*, 2010, **46**, 1088–1090; c) X. F. Zhang, R. Lu, J. H. Jia, X. L. Liu, P. C. Xue, D. F. Xu and H. P. Zhou, *Chem. Commun.*, 2010, **46**, 8419–8421.
9 P. C. Xue, B. Q. Yao, J. B. Sun, Z. Q. Zhang and R. Lu, *Chem. Commun.*, 2014, **50**, 10284–10286.
10 a) J. Seo, J. W. Chung, I. Cho and S. Y. Park, *Soft Matter*, 2012, **8**, 7617–7622; b) J. Lee, J. E. Kwon, Y. You and S. Y. Park, *Langmuir*, 2014, **30**, 2842–2851.
11 Z. Xie, V. Stepanenko, B. Fimmel and F. Würthner, *Mater. Horiz.*, 2014, **1**, 355–359.
12 E. Sheepwash, V. Krampl, R. Scopelliti, O. Sereda, A. Neels, and K. Severin, *Angew. Chem. Int. Ed.*, 2011, **50**, 3034 –3037.
13 a) X. F. Zhang, X. L. Liu, R. Lu, H. J. Zhang and P. Gong, *J. Mater. Chem.*, 2012, **22**, 1167–1172. b) Z. Ding, Q. Zhao, R. Xing, X. Wang, J. Ding, L. Wang and Y. Han, *J. Mater. Chem. C*, 2013, **1**, 786–792.
14 J. Lee, J. E. Kwon, Y. You and S. Y. Park, *Langmuir*, 2014, **30**, 2842−2851.
15 a) M. Shimizu, R. Kaki, Y. Takeda, T. Hiyama, N. Nagai, H. Yamagishi and H. Furutani, *Angew. Chem. Int. Ed.*, 2012, **51**, 4095–4099; b) P. C. Xue, J. B. Sun, P. Chen, P. Gong, B. Q. Yao, Z. Q. Zhang, C. Qian and R. Lu, *J. Mater. Chem. C*, 2015, **3**, 4086–4092.
16 T. H. Xu, R. Lu, X. L. Liu, P. Chen, X. P. Qiu and Y. Y. Zhao, *Eur. J. Org. Chem.*, 2008, 1065–1071.
17 N. M. Sangeetha and U. Maitra, *Chem. Soc. Rev.*, 2005, **34**, 821–836.
18 C. Y. Zhang, Y. K. Che, X. M. Yang, B. R. Bunes and L. Zang, *Chem. Commun.*, 2010, **46**, 5560–5562.
19 a) M. Kumar, N. Jonnalagadda and S. J. George, *Chem. Commun.*, 2012, **48**, 10948; b) T. Qi, V. Maurizot, H. Noguchi, T. Charoenraks, B. Kauffmann, M. Takafuji, H. Ihara and I. Huc, *Chem. Commun.*, 2012, **48**, 6337; c) P. C. Xue, B. Q. Yao, Y. Zhang, P. Chen, K. C. Li, B. J. Liu and R. Lu, *Org. Biomol. Chem.*, 2014, **12**, 7110–7118; d) F. C. Spano, *Acc. Chem. Res.*, 2010, **43**, 429–439.
20 P. Gong, P. C. Xue, C. Qian, Z. Q. Zhang and R. Lu, *Org. Biomol. Chem.*, 2014, **12**, 6134–6144.
21 a) X. L. Liu, D. F. Xu, R. Lu, B. Li, C. Qian, P. C. Xue, X. F. Zhang and H. P. Zhou, *Chem. Eur. J.*, 2011, **17**, 1660–1669; b) A. P. Sivadas, N. S. S. Kumar, D. D. Prabhu, S. Varghese, S. K. Prasad, D. S. S. Rao and S. Das, *J. Am. Chem. Soc.*, 2014, **136**, 5416–5423; c) H. Maeda, Y. Terashima, Y. Haketa, A. Asano, Y. Honsho, S. Seki, M. Shimizu, H. Mukai and K. Ohta, *Chem. Commun.*, 2010, **46**, 4559–4561; d) G. H. Hong, C. Qian, P. C. Xue, X. L. Liu, Q. Q. Wang, M. Y. Liu, P. Gong and R. Lu, *Eur. J. Org. Chem.*, 2014, 6155–6162; e) J. Gierschner and S. Y. Park, *J. Mater. Chem. C*, 2013, **1**, 5818–5832.
22 H. Ding, J. Sun, C. Wang, *Chin. J. Chem. Phys.*, 2012, **25**, 666–670.
23 a) K. K. Kartha, S. S. Babu, S. Srinivasan and A. Ajayaghosh, *J. Am. Chem. Soc.*, 2012, **134**, 4834–4841; b) L. Zang, Y. K. Che and J. S. Moore, *Acc. Chem. Res.*, 2008, **41**, 1596–1608.
24 a) L. Shi, C. He, D. Zhu, Q. He, Y. Li, Y. Chen, Y. Sun, Y. Fu, D. Wen, H. Cao and J. Cheng, *J. Mater. Chem.*, 2012, **22**, 11629; b) P. C. Xue, Q. X. Xu, P. Gong, C. Qian, A. M. Ren, Y. Zhang and Ran Lu, *Chem. Commun.*, 2013, **49**, 5838–5840.
25 P. C. Xue, J. B. Sun, B. Q. Yao, P. Gong, Z. Q. Zhang, C. Qian, Y. Zhang and R. Lu, *Chem. Eur. J.*, 2015, **21**, 4712–4720.

Graphic Abstract for:

Strong blue emissive nanofibers constructed from benzothizole modified *tert*-butyl carbazole derivative for the detection of volatile acid vapors

Luminescent nanofibers were fabricated from nontraditional π-gelator and used as fluorescence sensor for detecting acid vapors.